Supplementary Table

Table S1. Comparison of the *Tm*LamCD models in different space groups. RMSD (Å) values on the upper-right were calculated by PDBeFold.

	1	2	3	4	5	6	7	8	9	10	11
1		0.43	0.60	0.35	0.42	0.46	0.48	0.63	0.43	0.39	0.36
2			0.74	0.44	0.24	0.39	0.58	0.77	0.29	0.21	0.45
3				0.68	0.73	0.76	0.75	0.35	0.74	0.72	0.71
4					0.41	0.42	0.36	0.65	0.38	0.41	0.23
5						0.38	0.55	0.76	0.27	0.19	0.41
6							0.45	0.77	0.30	0.37	0.40
7								0.68	0.47	0.54	0.37
8									0.75	0.75	0.66
9										0.27	0.35
10											0.41
11											

1, chain A, open form, in $P2_12_12_1$; 2, chain A, closed form, in $P2_12_12_1$; 3, chain B in $P2_12_12_1$; 4, chain C in $P2_12_12_1$; 5, chain D in $P2_12_12_1$; 6, chain A in *C*2; 7, chain B in *C*2; 8, chain A in $P4_3$; 9, chain B in $P4_3$; 10, chain C in $P4_3$; 11, chain D in $P4_3$

Supplementary Figure Legends

Fig. S1. The topology of the (A) *Tm*LamCD and (B) *Tm*Cel12A. The secondary structure is generated by the ESPript software. The η denotes 3_{10} helix.

Fig. S2. Stereoview of a double occupancy of the flexible GASIG loop was observed in some *Tm*LamCD chains. (A) The difference Fourier map (mF_o-DF_c) of the GASIG loop is shown in gray mesh contoured at 1.5σ. (B) The flexible GASIG fragment in the *Tm*LamCD coordinate. The closed configuration is shown in hot pink, and the open form is in cyan.

Fig. S3. Steroview of superimposed Cα traces of catalytic domains of laminarinase structures. Chain A was selected for each structure to compare the diversity. 2HYK is shown in blue, 2VY0 in green, 3ILN in orange, 3DGT in cyan, *Tm*LamCD with the open form loop in magenta and closed form loop in red. Variable regions of the secondary structures are labeled according to the annotation in Fig.1B.

Fig. S4. Ligplot of gluconolactone complexed in laminarinase showing H-bonds and hydrophobic interactions around the active site. Lgc represents gluconolactone, and 16A means cetyltrimethylammonium (ctab) molecule. A, B, C in the parenthesis means the chain code in the asymmetric unit. (D) The ligplot shows the amino acid residues around the inhibitor with hydrophobic contacts.

Fig. S5. Electrostatic potential surface diagram of *Tm*Lam catalytic domain shows the charge character of the catalytic groove. (A) A modeled long chain β-1,3-glucan moves outwards the active site of *Tm*LamCD. (B) Modeled laminarihexaose penetrates the entranceway of the *Tm*LamCD. Negative potentials are colored in red, positive in blue, and neutral in white. Ligands are shown in green sticks.

Fig. S6. Calcium coordinates. (A) Stereo image of the surrounding Lam residues coordinating with the calcium ion (chocolate). Calcium coordinates are shown in green. (B) Ligplot to show each distance of coordinates in green.

Fig. S7. Structural comparison of the catalytic grooves among glucanases or the carbohydrate binding module. (A) A laminarihexaose molecule was bound on the carbohydrate-binding module of *T. maritima* laminarinase (PDB: 1GUI) (27). (B) A cellotetraose locates in the cellulase12A from *T. maritima* (PDB of TmCel12A: 3AMM) (35). (C) An exo-β-1,3-glucanase from *Candida albicans* in complex with laminaritriose (PDB: 3N9K) (D) A *p*-nitrophenyl-β-D-glucopyranoside molecule located in the β-glucosidase E193D mutant protein from *Neotermes koshunensis* (PDB of *Nk*Bgl-E193D-*p*NPG: 3AI0) (37). Figures on the left represent the surface view, and the detailed interactive residues are shown on the right ones. All ligands are shown in thick stick. Protein residues interacting with ligands by electrostatic forces are shown in yellow sticks, whereas hydrophobic interacting residues are in magenta. Potential interactive residues are in cyan. Hydrogen bonds are indicated by dashed lines.

Fig. S8. Comparison of *Tm*LamCD and *Tm*Cel12A strcutures. (A) Overlay of chain A of both *Tm*LamCD (in cyan) and *Tm*Cel12A structures (in gray) by superposing residues 123-140 (in yellow) of *Tm*LamCD with residues 126-143 of *Tm*Cel12A. (B) and (C) represent the surface view of the substrate-binding cleft of *Tm*LamCD and *Tm*Cel12A, respectively. The gluconolactone, laminaritriose, and cellotetraose molecules are shown in cyan, blue and purple sticks.

Fig. S9. Thin-layer chromatography of the digested products of laminarin by *Tm*LamCD. Glucose (G1, lane1), maltose (G2, lane 2), laminaritriose (G3, lane 3) and laminaritetraose (G4, lane 4) were used as standards. Five μg *Tm*LamCD protein were used to digest 2.4% laminarin in 25 mM sodium phosphate buffer (pH 7.0) at 45°C for 30 sec (lane 5), 1 min (lane 6), 5 min (lane 7) and 18 hours (lane 8). Lane 9 and lane 10 represent controls as 5% laminarin without *Tm*LamCD and 5 mg

*Tm*LamCD without laminarin, respectively, in 25 mM sodium phosphate buffer (pH 7.0) at 45^{o}C for 18 hours. Solutions of lanes 1-4, 8, and 9 were frozen before TLC analysis.

Fig. S10. A modeled long chain laminarin at the reducing end of carbohydrate in the *Tm*LamCD catalytic cavity. Subsites of glucosyl residues in the active site are numbered in black. Amino acid residues around the enclosure at the catalytic cavity of TmLamCD are labeled in gray.

Fig. S11. Superimposed Cα traces of catalytic domains of laminarinase structures. 2HYK is shown in blue, 2VY0 in green, 3ILN in orange, open form of *Tm*LamCD in magenta, and the closed form GASIG loop of *Tm*LamCD in red. Side chains of Trp residues corresponding to Trp232 in TmLamCD are shown in sticks and numbered according to their deposited PDB. (A) Stereoview of the superimposed structures shown in cartoon loop. (B) Surface view of each structure showing their catalytic cavity.

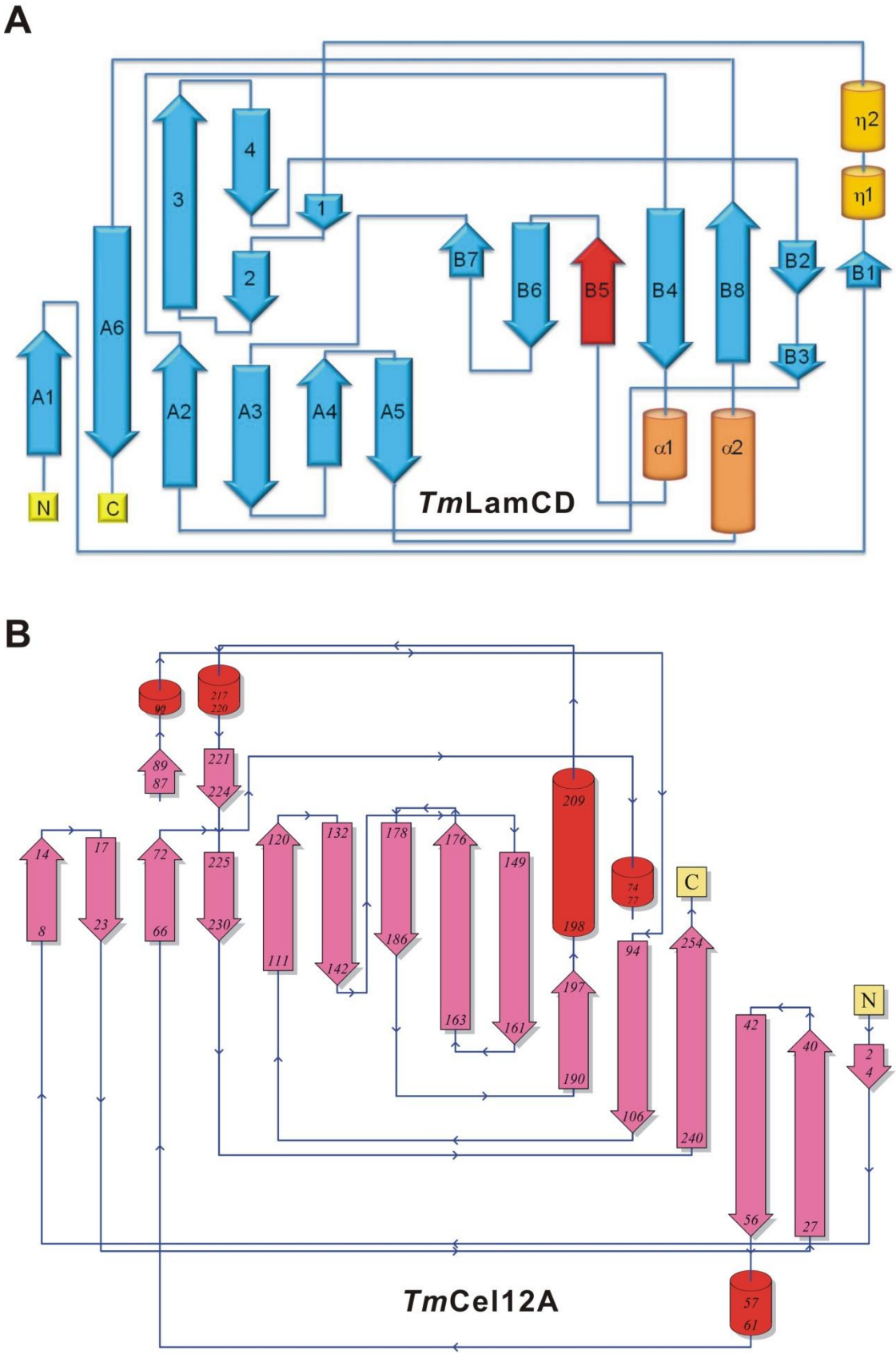
A
η2
η1
4
3
1
B7
B6
B5
B4
B8
B2
B1
2
A6
B3
A1
A2
A3
A4
A5
α1
α2
N
C
TmLamCD
B
C
N
TmCel12A

Figure S1

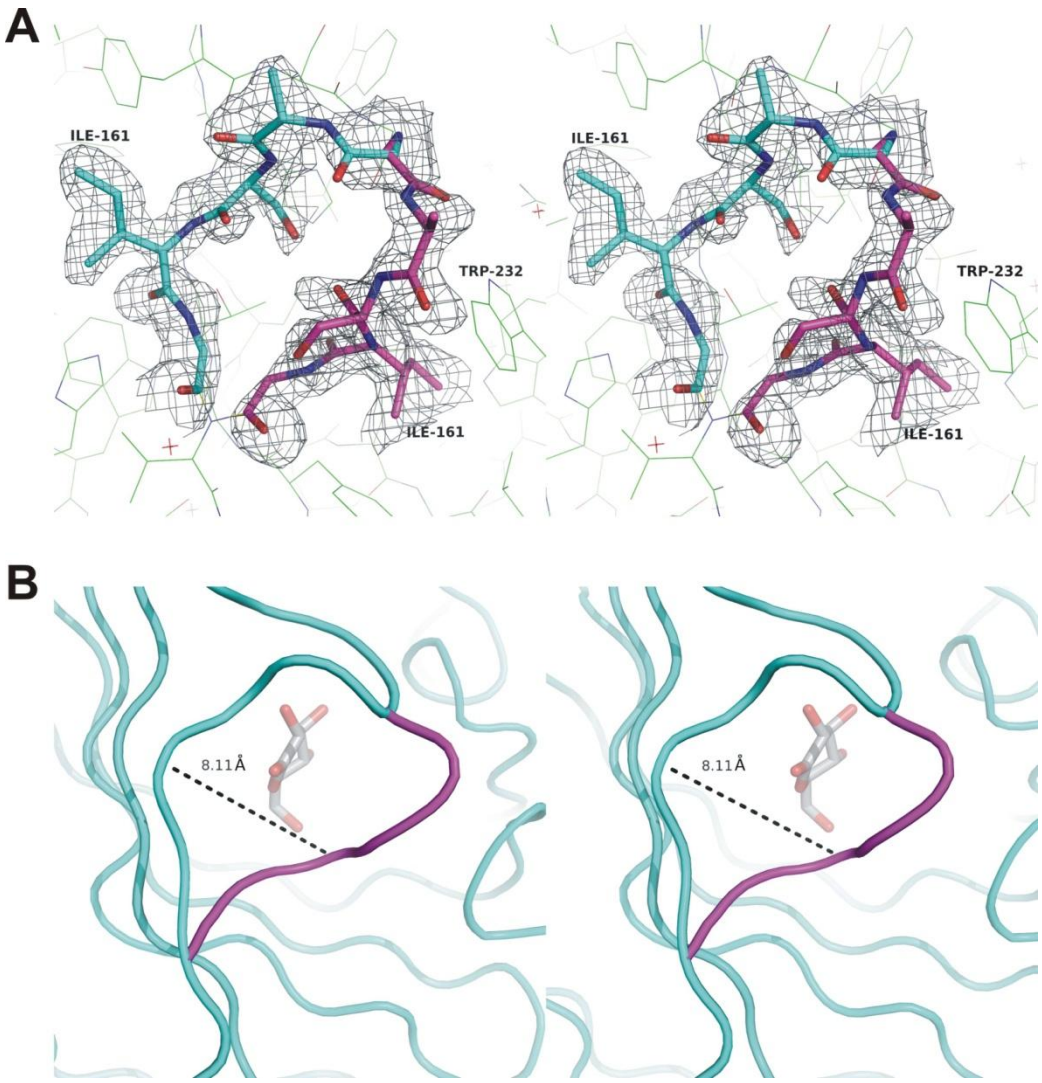

Figure S2

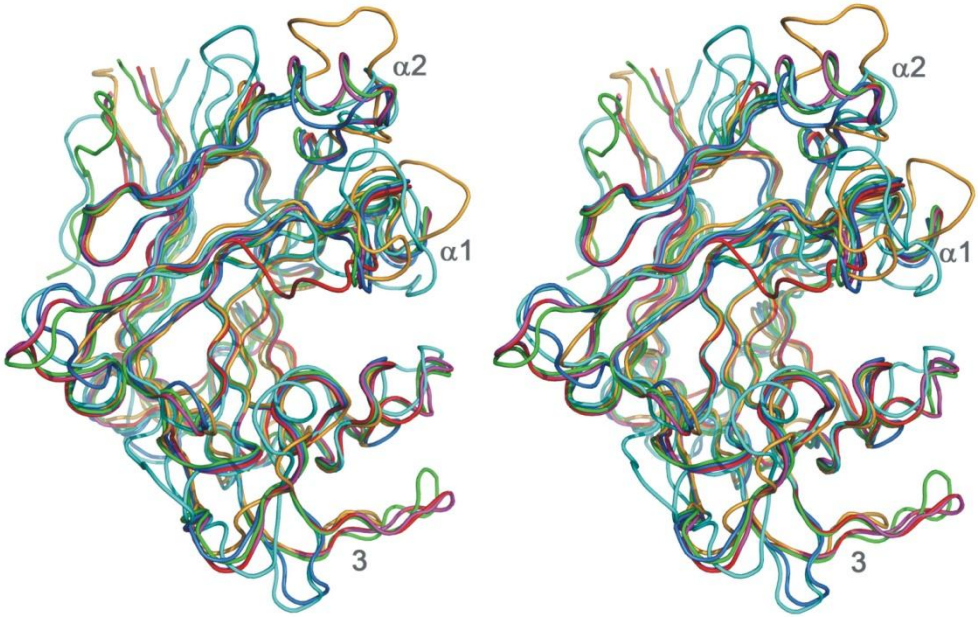

Figure S3

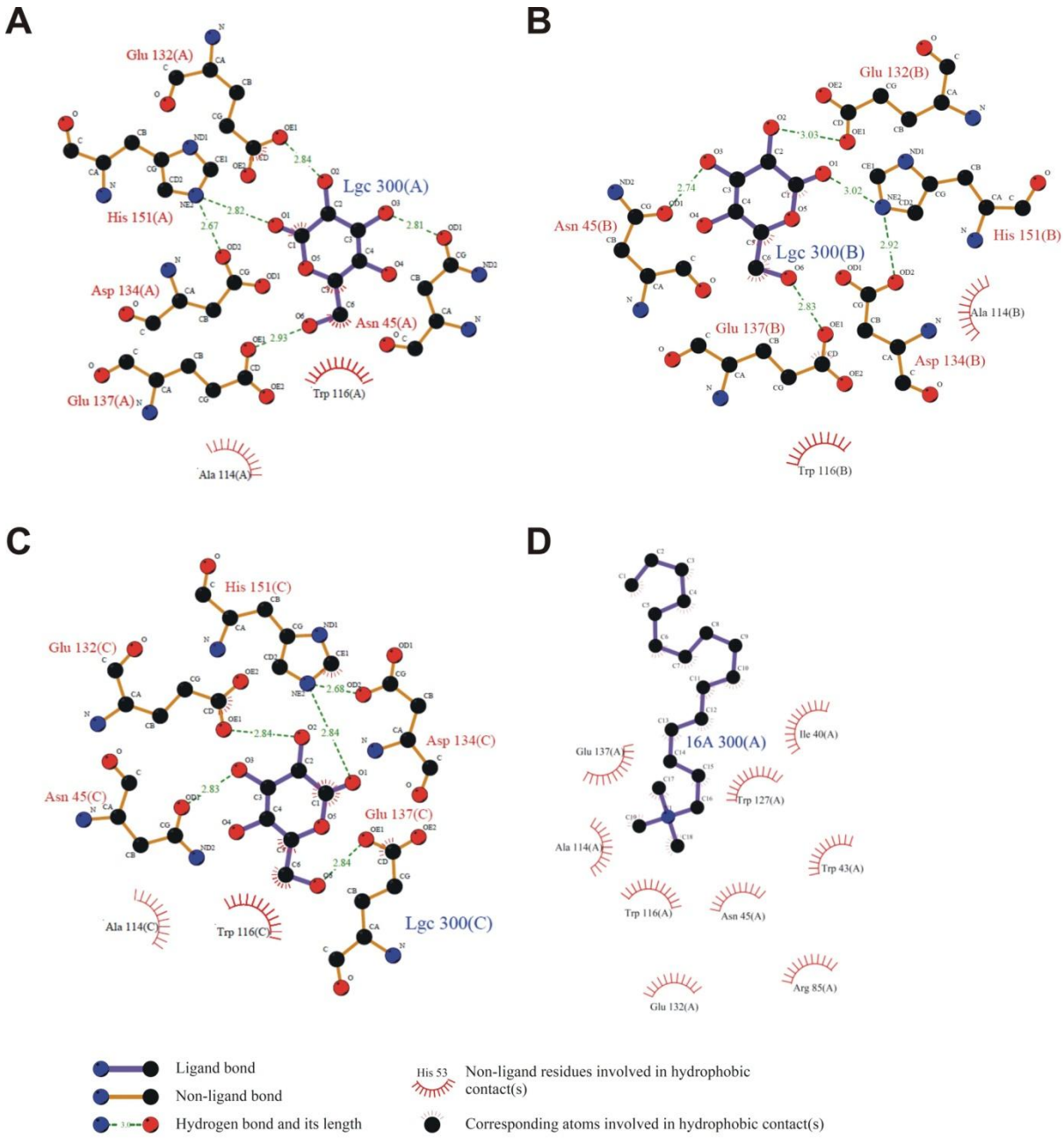
A
Glu 132(A)
Lgc 300(A)
His 151(A)
Asp 134(A)
Asn 45(A)
Glu 137(A)
Trp 116(A)
Ala 114(A)
B
Glu 132(B)
Asn 45(B)
Lgc 300(B)
His 151(B)
Ala 114(B)
Glu 137(B)
Asp 134(B)
Trp 116(B)
C
His 151(C)
Glu 132(C)
Asp 134(C)
Asn 45(C)
Glu 137(C)
Lgc 300(C)
Ala 114(C)
Trp 116(C)
D
16A 300(A)
Glu 137(A)
Ile 40(A)
Trp 127(A)
Ala 114(A)
Trp 43(A)
Trp 116(A)
Asn 45(A)
Arg 85(A)
Glu 132(A)
Ligand bond
Non-ligand bond
Hydrogen bond and its length
His 53
Non-ligand residues involved in hydrophobic contact(s)
Corresponding atoms involved in hydrophobic contact(s)

Figure S4

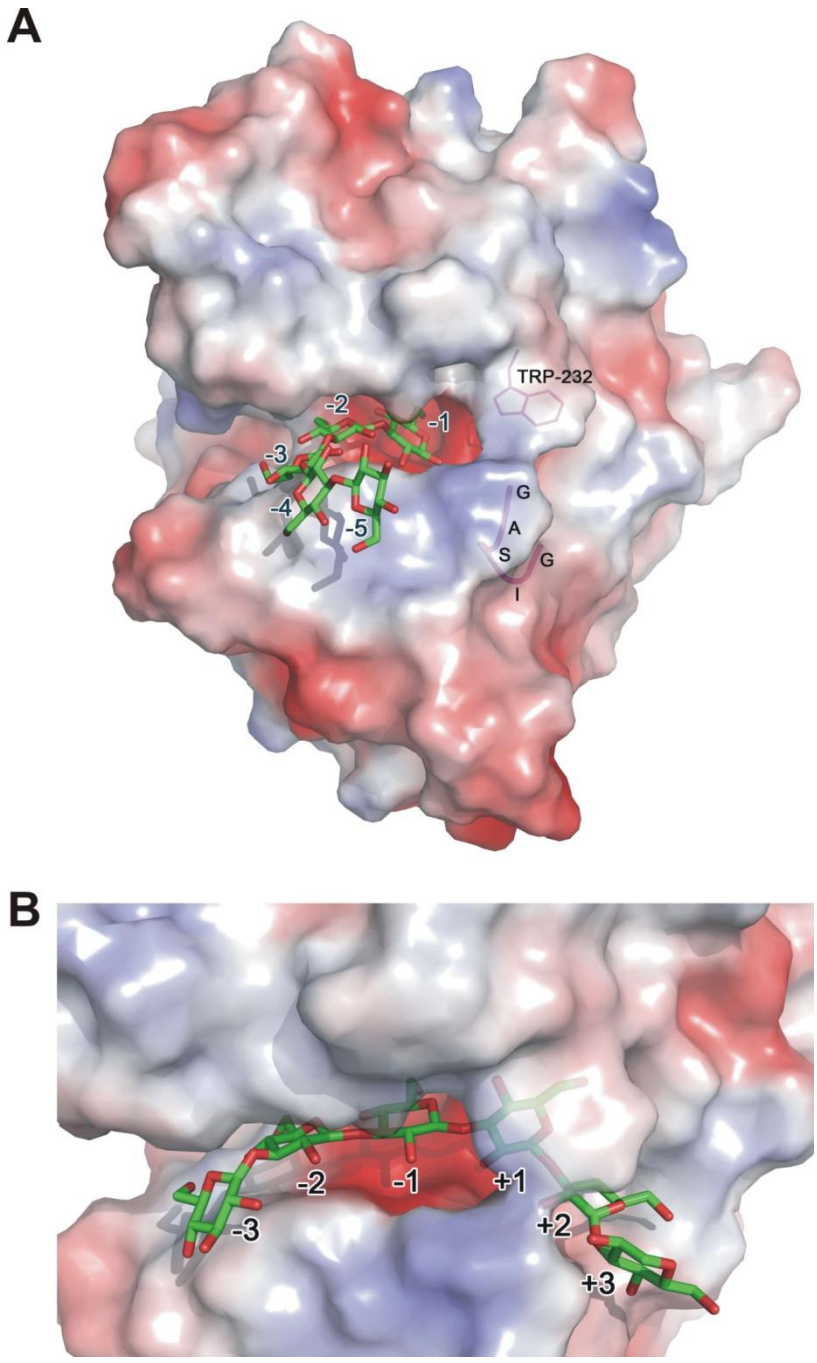

Figure S5

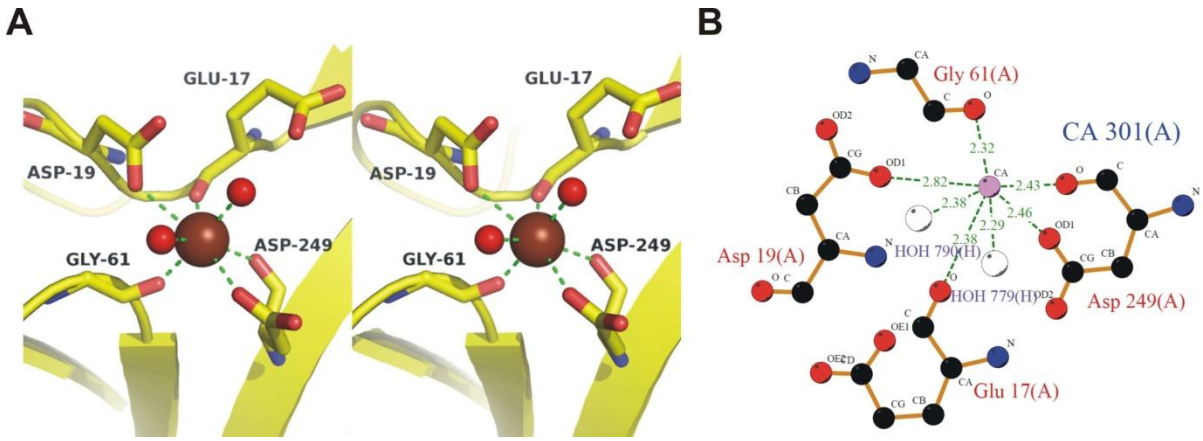
A
GLU-17
ASP-19
GLY-61
ASP-249
GLU-17
ASP-19
GLY-61
ASP-249
B
Gly 61(A)
CA 301(A)
Asp 19(A)
HOH 790(H)
HOH 779(H)
Asp 249(A)
Glu 17(A)

Figure S6

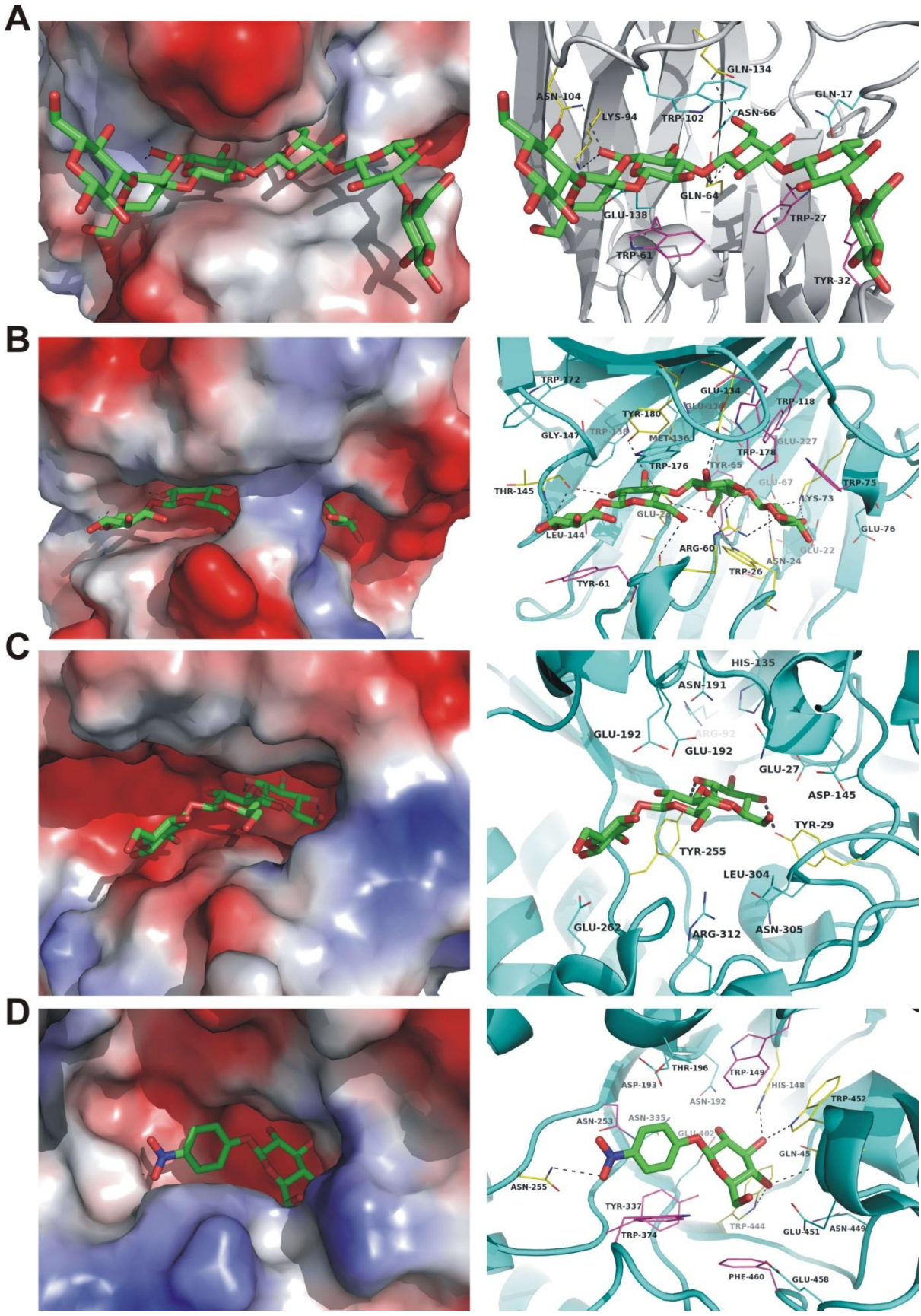
A
GLN-134
ASN-104
GLN-17
LYS-94
TRP-102
ASN-66
GLN-64
GLU-138
TRP-27
TRP-61
TYR-32
B
TRP-172
GLU-134
TRP-118
TYR-180
GLY-147
MET-136
GLU-227
TRP-178
TRP-176
TYR-65
GLU-67
TRP-75
THR-145
LYS-73
LEU-144
GLU-76
ARG-60
GLU-22
ASN-24
TRP-26
TYR-61
C
HIS-135
ASN-191
GLU-192
GLU-192
GLU-27
ASP-145
TYR-29
TYR-255
LEU-304
GLU-262
ARG-312
ASN-305
D
THR-196
TRP-149
ASP-193
HIS-148
ASN-192
TRP-452
ASN-253
ASN-335
GLN-45
ASN-255
TYR-337
TRP-444
GLU-451
ASN-449
TRP-374
PHE-460
GLU-458

Figure S7

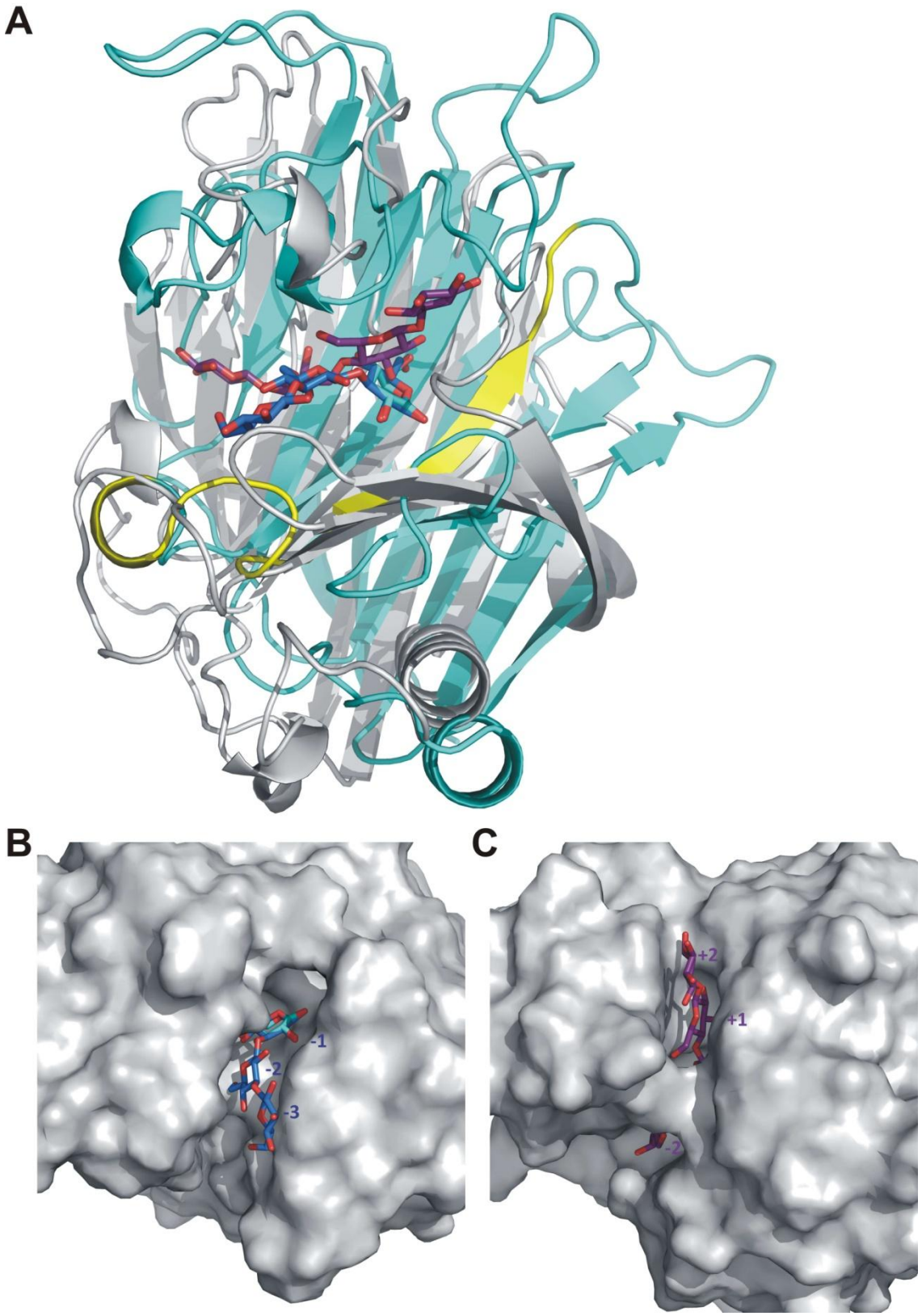

Figure S8

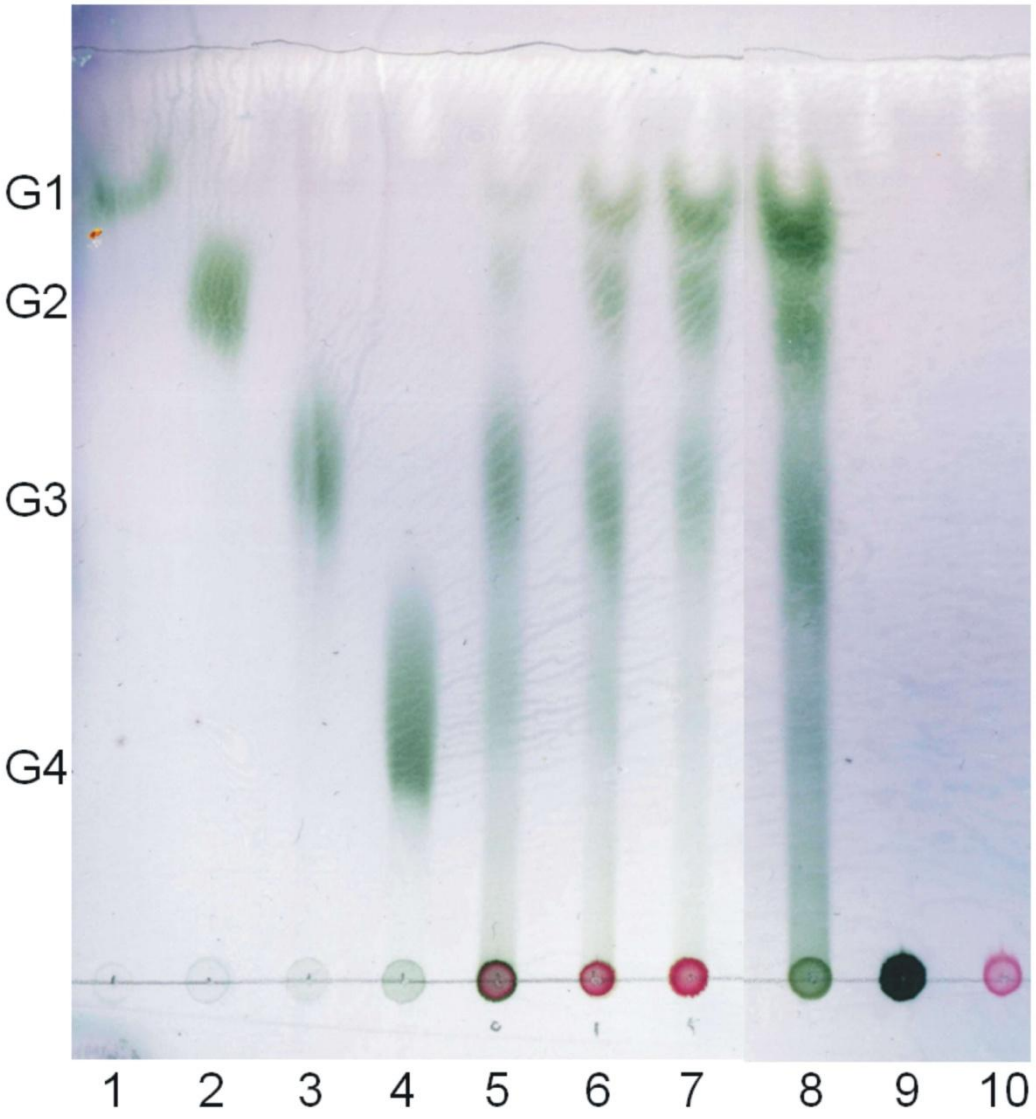

Figure S9

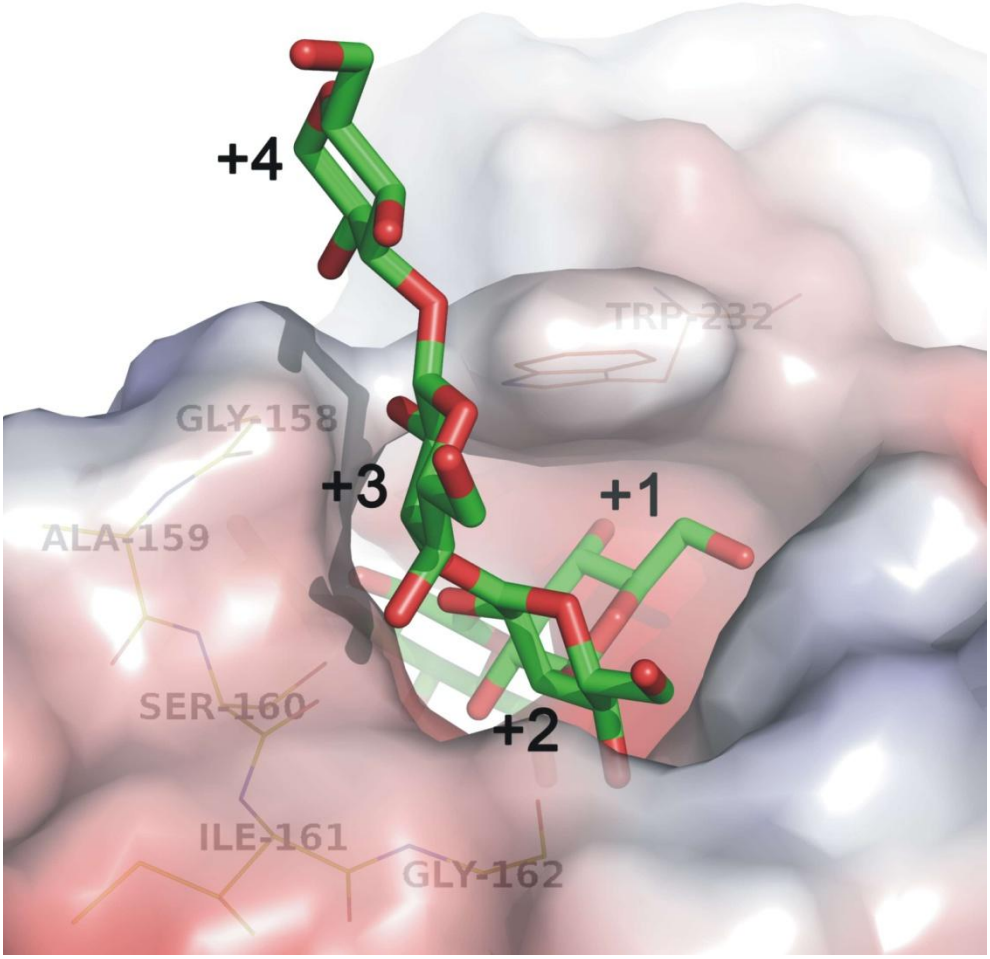

Figure S10

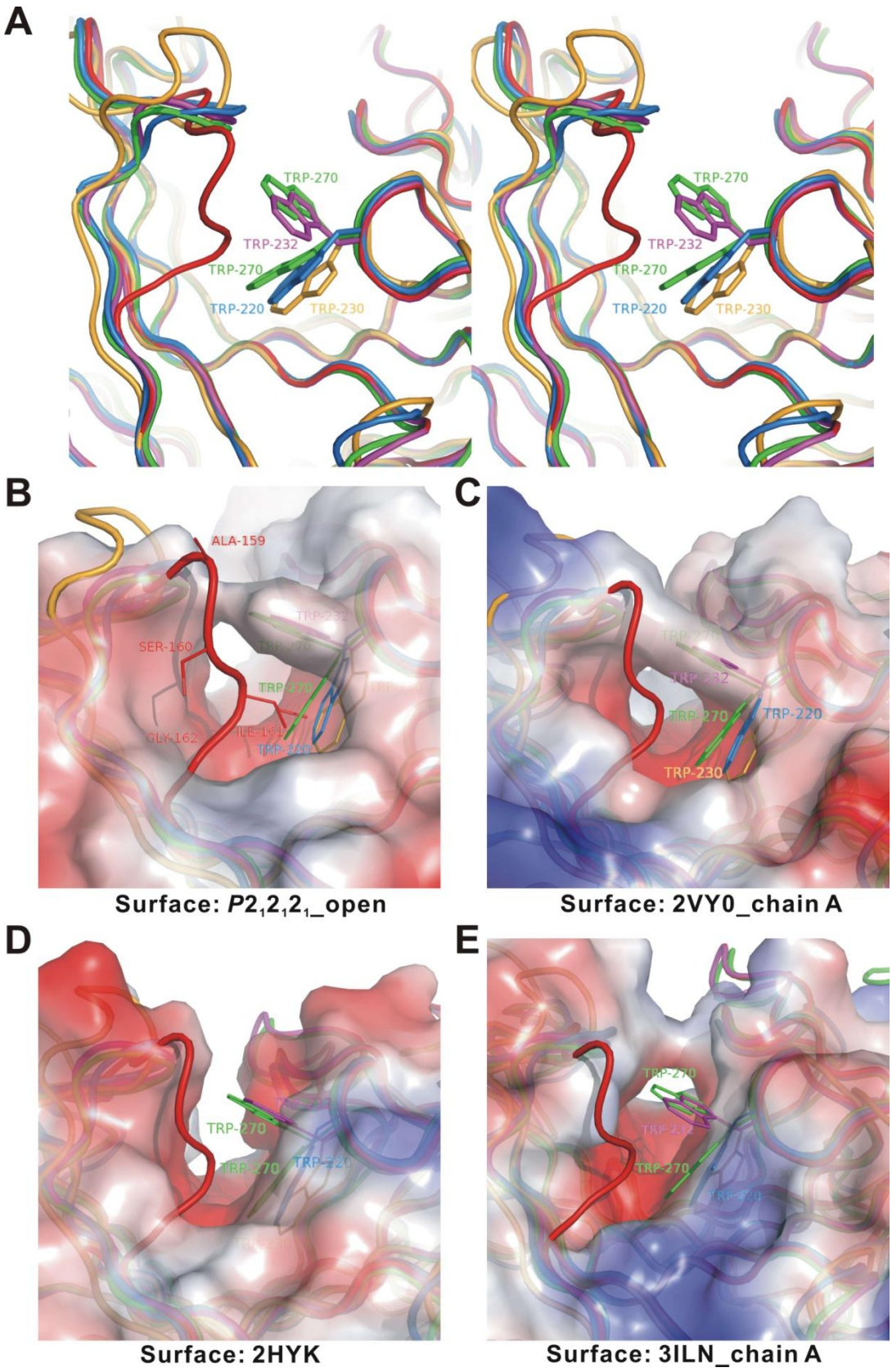
A
TRP-270
TRP-232
TRP-270
TRP-220
TRP-230
TRP-270
TRP-232
TRP-270
TRP-220
TRP-230
B
ALA-159
SER-160
GLY-162
TRP-270
TRP-220
Surface: P2₁2₁2₁_open
C
TRP-232
TRP-270
TRP-220
TRP-230
Surface: 2VY0_chain A
D
TRP-270
TRP-270
TRP-220
Surface: 2HYK
E
TRP-270
TRP-270
Surface: 3ILN_chain A

Figure S11